NASA TECHNICAL MEMORANDUM

NASA TM X-3269

NASA TM X-3269

ACCELERATED LIFE TEST OF SPUTTERING AND ANODE DEPOSIT SPALLING IN A SMALL MERCURY ION THRUSTER

John L. Power

Lewis Research Center

Cleveland, Ohio 44135

NATIONAL AERONAUTICS AND SPACE ADMINISTRATION • WASHINGTON, D. C. • SEPTEMBER 1975

1. Report No.	2. Government Accession No.	3. Recipient's Catalog No.
NASA TM X-3269		

4. Title and Subtitle	5. Report Date
ACCELERATED LIFE TEST OF SPUTTERING AND ANODE DEPOSIT SPALLING IN A SMALL MERCURY ION THRUSTER	September 1975
	6. Performing Organization Code
7. Author(s)	8. Performing Organization Report No.
John L. Power	E-8152
	10. Work Unit No.
9. Performing Organization Name and Address	506-22
Lewis Research Center National Aeronautics and Space Administration Cleveland, Ohio 44135	11. Contract or Grant No.
	13. Type of Report and Period Covered
12. Sponsoring Agency Name and Address	Technical Memorandum
National Aeronautics and Space Administration Washington, D.C. 20546	14. Sponsoring Agency Code

15. Supplementary Notes

16. Abstract

Tantalum and molybdenum sputtered from discharge-chamber components during operation of a 5-centimeter-diameter mercury ion thruster adhered much more strongly to coarsely grit-blasted anode surfaces than to standard smooth surfaces. Spalling of the sputtered coating did occur from a coarse screen anode surface but only in flakes less than a mesh unit long. The results were obtained in a 200-hour accelerated life test conducted at an elevated discharge potential of 64.6 volts. The test approximately reproduced the major sputter erosion and deposition effects that occur under normal operation but at approximately 75 times the normal rate. No discharge-chamber component suffered sufficient erosion in the test to threaten its structural integrity or further serviceability. The test indicated that the use of tantalum-surfaced discharge-chamber components in conjunction with a fine-wire-screen anode surface should cure the problems of sputter erosion and sputtered deposit spalling in long term operation of small mercury ion thrusters.

17. Key Words (Suggested by Author(s))	18. Distribution Statement
Spalling; Sputtering; Ion engine; Mercury vapor; Deposition; Deposits; Erosion; Flakes; Flaking	Unclassified - unlimited STAR Category 20 (rev.)

19. Security Classif. (of this report)	20. Security Classif. (of this page)	21. No. of Pages	22. Price*
Unclassified	Unclassified	40	$3.75

* For sale by the National Technical Information Service, Springfield, Virginia 22161

ACCELERATED LIFE TEST OF SPUTTERING AND ANODE DEPOSIT SPALLING IN A SMALL MERCURY ION THRUSTER

by John L. Power

Lewis Research Center

SUMMARY

In an accelerated life test sputtered tantalum and molybdenum from the discharge-chamber components of a 5-centimeter-diameter mercury ion thruster adhered strongly to grit-blasted tantalum and stainless-steel anode surfaces and moderately well to a coarse stainless-steel screen anode surface. No spalling of the coatings on the grit-blasted surfaces or cracks in them occurred, and only minute, partial-mesh-unit-length coating flakes spalled from the screen surface.

The sputter-erosion and deposition rates of the discharge-chamber components were greatly accelerated by operating the thruster at the abnormally high discharge potential ΔV_I of 64.6 volts. The test was conducted continuously for 200 hours at otherwise standard 5-centimeter-thruster operating conditions. From a comparison of the measured baffle and estimated screen-grid erosion with previous data, it is estimated that the discharge-chamber sputter erosion and deposition in the test was equivalent to that occurring in approximately 15 000 hours of normal operation at $\Delta V_I = 39.6$ volts.

The experiment indicated that, by employing a grit-blasted, fine-mesh-screen anode and using tantalum for all exposed surfaces of the other discharge-chamber components (apart from the molybdenum screen grid), no problems due to flaking of sputtered deposits should occur in small mercury ion thrusters over operational lifetimes in excess of 15 000 hours.

The test also indicated that the sputter erosion occurring in 15 000 hours of operation at a normal discharge potential would not threaten the structural integrity or serviceability of any discharge-chamber component in the ion engine tested.

INTRODUCTION

A 9715-hour endurance test of a standard 5-centimeter-diameter mercury ion en-

gine (SIT-5) was terminated because large flakes of sputter-deposited material spalled from the anode and collected on the screen grid (ref. 1). This thruster used a smooth, polished stainless-steel anode and several other discharge-chamber components having exposed iron or stainless-steel surfaces.

The flakes that had spalled from the anode in the endurance test (ref. 2) were not from the thickest part of the anode coating. On their under surfaces they showed a high molybdenum content and were quite smooth. A plausible mechanism advanced (ref. 2) for the spalling of the flakes from the anode attributed it to the differential expansion and contraction of the molybdenum-rich under surfaces of the flakes and the stainless-steel substrate during thruster thermal cycling. It was suggested that the smoothness of both surfaces aggravated the spalling process.

Three 400-hour SIT-5 tests at discharge potentials ΔV_I of 36.6, 39.6, and 42.6 volts revealed that the sputter erosion rates of the discharge-chamber components were generally increased by a factor of about 5 over this 6-volt range of ΔV_I (ref. 2). The relative erosion rates in the three tests correlated with the theoretical increase in doubly charged mercury ion (Hg^{+2}) production over the same range of ΔV_I. Based on these results, B. A. Banks of Lewis suggested that an accelerated life test of discharge-chamber sputtering, anode deposition, and anode deposit spalling could be accomplished by steady-state thruster operation at a higher ΔV_I than normal.

The experiment reported in this report was undertaken in an attempt to evaluate potential solutions to the combined problems of sputtering and sputtered deposit spalling over a simulated mission lifetime for a small mercury ion thruster. The experiment had three objectives. One was to test how well the accelerated life test concept could reproduce the sputter erosion and the deposition and spalling of sputtered material that occur in the discharge chamber during normal, long-term uncycled thruster operation. The second was to test the effectiveness, during such an accelerated life test, of novel anode surfaces in improving the adhesion of sputtered material deposited on the anode and in preventing the spalling of large flakes of such deposited coatings. Screen and grit-blasted anode surfaces were proposed by Banks for testing under this objective. The third objective of the experiment was to evaluate the potential benefits of preparing from one sputter-resistant material all the discharge chamber surfaces subject to sputter erosion. Part of this objective was also to determine if the integrity and serviceability of any discharge-chamber component was threatened due to sputter erosion during long-term thruster operation.

APPARATUS

Thruster

A scale drawing of the 5-centimeter-diameter thruster is shown in figure 1. The

thruster and cathodes, including the electrostatic vector grid system, were the same as those used in the SIT-5 erosion studies (refs. 2 and 3) except for the following changes:

(1) Two 0.05-millimeter-thick tantalum foil covers were installed over the exposed mild steel cathode pole-piece surfaces (figs. 1 and 2).

(2) The long, SIT-5 baffle support system stainless-steel screw and nut extending into the discharge chamber (ref. 2) were replaced by a tantalum screw having a thin head on the discharge chamber side (figs. 1 and 3).

(3) A 0.50-millimeter-thick tantalum cover was installed over the interior surface of the thruster endplate.

(4) A composite anode having five different interior surfaces was used. Figures 4 and 5 show the anode layout and assembly. The individual anode surfaces, each extending over virtually the entire length of the anode, were as follows:

(a) The virgin, smooth stainless-steel surface of the anode shell, exposed over an arc of 41.5°.

(b) The same surface uniformly grit-blasted with a 50-micrometer-particle-size silicon carbide abrasive powder, using a micro-sandblaster. This surface (fig. 6) was exposed over an arc of 37°. An electron micrograph of the surface (fig. 7) indicates its extreme roughness and micro-angularity. Typical surface features on it are 10 micrometers across and about equally deep.

(c) A coarse, opaque, double woven stainless-steel screen (20 by 100 wires cm), made of 0.20- to 0.25-millimeter-diameter wire and having surface mesh opening dimensions (measured between wire center lines) of approximately 0.40 by 0.50 millimeter. This surface was exposed over an arc of 163.5°. A magnified picture of the screen surface is shown in figure 8.

(d) The virgin, smooth surface of a 0.05-millimeter-thick tantalum foil insert, exposed over an arc of 59°.

(e) The same surface (part of the same insert) grit-blasted as above and exposed over an arc of 59°. Figure 9 shows both the grit-blasted and the smooth surfaces of the insert.

(5) The SIT-5 anode pole-piece insert was reused after the exposed interior surfaces of nickel-plated iron had been plasma-spray coated with tantalum to a thickness of 0.075 to 0.10 millimeter. The tightly adhering coating obtained had a rough, granular surface (fig. 10) and covered the critical insert tip edge without any obvious flaws.

(6) A replacement neutralizer of the Hughes design (ref. 4), believed identical to the one used during the previous thruster tests, was used.

One consequence of the parts and materials changes was that, except for the molybdenum screen grid, only tantalum surfaces were exposed to sputter erosion in the discharge chamber. However, the stainless-steel baffle support wires and portions of the mild steel cathode pole piece were exposed to the discharge upstream of the baffle. This

portion of the discharge is not technically part of the main discharge.

All discharge-chamber components were carefully and thoroughly cleaned in an ultrasonic bath, using 1, 1, 1 trichloroethane as the solvent, before final assembly. The parts were then protected from fingerprints and other surface contamination during assembly and installation of the thruster and during disassembly of the thruster following completion of the test.

Power Processor

The power processing and control package used to operate the thruster was the same as that used during the SIT-5 erosion tests (ref. 5) except that the proportional feedback control circuit that controls the main cathode flow rate by means of the current to the main vaporizer was modified. The control circuit was altered so as to sense and control on the basis of the parameter $(\Delta V_I - V_{CK})$, where V_{CK} is the cathode keeper potential, instead of on ΔV_I. This modification allowed the beam current J_B to be held constant at the required level at the same time that the control circuit automatically adjusted the mercury flow rate to keep $(\Delta V_I - V_{CK})$ constant at the desired preset value.

This circuit modification was made because of previous observations in SIT-5 thruster tests that $(\Delta V_I - V_{CK})$ was insensitive to V_{CK} fluctuations but that ΔV_I was very sensitive to such fluctuations. In these observations random, fast V_{CK} fluctuations (usually increases of 1- to 3-V amplitude lasting a few seconds) occurred frequently, for unknown reasons, and caused corresponding fluctuations of the same magnitude and sign with no time lag in ΔV_I. These in turn resulted in unacceptable variations in the main cathode mercury flow rate as the control circuit responded to the rapidly varying ΔV_I.

The identical, coincident fluctuations noted in V_{CK} and ΔV_I indicate that the main discharge plasma in the SIT-5 thruster is strongly coupled from the cathode keeper potential to the anode potential. This was previously found by Bechtel (ref. 6) in the 30 centimeter mercury ion thruster as well. Hence, the main discharge operates through a potential drop given by $(\Delta V_I - V_{CK})$. The observed V_{CK} fluctuations evidently were fluctuations only in the potential drop across a plasma sheath at the cathode tip and were not transmitted to the main discharge.

RESULTS AND DISCUSSION

Thruster Operation

The thruster operated continuously without difficulties or shutdowns during the

200-hour test. Characteristic thruster operating values maintained during the test are shown in table I. The controllable parameters were held at the same levels as during the SIT-5 erosion tests (ref. 2), except for ΔV_I and the neutralizer flow rate. Because of poor neutralizer operation, an excessively high neutralizer flow rate was required during the 200-hour test to maintain an adequately low neutralizer coupling voltage.

Throughout the test the thruster operated very smoothly and stably in the autocontrol mode, controlling on $(\Delta V_I - V_{CK})$. Apart from short-term fluctuations (<20 sec), ΔV_I remained within ±0.2 volt of the desired 64.6 volts throughout the test, with the beam current J_B maintained at 23.4 microamperes. The value of 64.6 volts for ΔV_I was chosen from preliminary tests, which indicated that 65 volts was the highest ΔV_I at which the thruster could be operated stably.

During startup and shutdown of the thruster, the accelerating voltages V_I and V_A were turned on immediately after the main discharge was started and turned off at the same time that the main discharge was extinguished. This procedure was followed to avoid any anomalously intense sputtering that might occur in the discharge chamber with the main discharge on but the high voltages off.

Sputter Erosion in Discharge Chamber

The weight changes found for the discharge-chamber components that lost weight during the test are compiled in table II. The grid assembly was the single most heavily eroded component, with the tantalum-foil cathode pole-piece tip cover next and the baffle third. A 1.1-milligram discrepancy in table II between the measured weight loss of the cathode pole-piece and baffle assembly (including the tantalum pole-piece covers) and the sum of the weight losses of the individual disassembled parts is believed to be due mainly to loose flakes and other material in the assembly that was lost on disassembling it.

The cathode pole-piece tip cover showed severe erosion around its inside diameter, both on its downstream flat surface and on its interior conical surface. Some of this erosion may be seen in figure 11. Three out of four of the 0.05-millimeter-thick (tantalum) tabs connecting the pieces composing these two surfaces were sputter eroded through and severed where they were bent over the downstream interior edge of the pole piece (see fig. 11). Sputtering of this thickness of tantalum during the test corresponds to a weight loss per unit area of at least 84 milligrams per square centimeter at the cathode pole-piece tip. The pole-piece tip cover as a whole lost 33 percent of its original weight during the test.

The cathode pole-piece outer-flange cover showed little erosion and no areas of localized high erosion after the test. This cover lost 3 percent of its weight in the test.

The only portion of the cathode pole piece proper exposed to the main discharge was the web structure forming the flow diversion slots, which are covered with a tantalum screen (100-mesh, 0.05-mm-diam wire). The screen material appeared relatively unaffected by the test, but the mild steel of the web outer surfaces showed apparently heavy sputter erosion.

The tantalum baffle showed heavy, quite uniform sputter erosion over its exposed downstream surface (figs. 12 and 13). The edge view in figure 12 shows the step between the exposed outer portion of this surface and the inner area that was shielded by the head of the baffle screw. Significant erosion of the exposed upstream baffle surface was also observed (see fig. 14). This observation was contrary to the SIT-5 erosion test results, in which no upstream surface erosion of the baffle was found (ref. 2).

In all, approximately 10 percent of the initial baffle weight was sputtered away in the accelerated life test. The baffle thickness near its outside diameter was reduced by 0.079 millimeter, or 13 percent of its initial thickness of 0.59 millimeter. The baffle outside diameter was reduced by 0.081 millimeter, or 1.3 percent of its initial 6.33 millimeters. From these dimension changes, assuming linear sputter erosion of the baffle with thruster operating time, it is clear that the baffle could survive intact through several times the equivalent operating time of the accelerated life test without a major loss in its outside diameter. However, even the dimension changes noted may be related to a significant change observed in the thruster operating characteristics during the test, namely, the monotonic increase required in the emission current J_E to maintain J_B at its standard value.

The tantalum baffle screw displayed heavy erosion of its exposed head, located on the downstream side of the baffle, with a loss in overall length of 0.10 millimeter. This loss in length is presumed to have been essentially all from the erosion of the downstream head surface.

Under the approximation that all the weight erosion of both the baffle and the baffle screw took place on their exposed downstream surfaces, the weight loss per unit area exposed was 118 milligrams per square centimeter for the baffle screw (head) and 107 milligrams per square centimeter for the baffle. This indicates fairly uniform sputter erosion across the downstream baffle-screw head surface at a rate comparable with that indicated for the most severely sputtered portions of the tantalum cathode pole piece tip cover.

The baffle washer and nut, both located upstream of the baffle, each showed a small but significant weight loss in the accelerated life test.

The tantalum endplate cover displayed little evidence of erosion and no reduction in thickness at the midradius of its exposed area. However, it did show a prominent imprint of the cathode pole-piece assembly that was mounted on top of it (see fig. 15). This imprint was due to net deposition of sputtered tantalum from the cathode pole-piece

outer flange cover on the exposed portion of the endplate cover surface immediately adjacent to the outer edges of the flange cover.

Several distinct types of erosion of the electrostatic vector grid system were indicated in the test. General surface erosion of the upstream screen grid surface was evident from its appearance, but some localized deposition and flake generation was also found on it. The deposition and flaking are described later. There was no evident erosion of the downstream screen grid surface. As is evident from the photographs taken before and after the test, the accelerator grid system (fig. 16) suffered minimal additional charge-exchange erosion of its charge-exchange pads. This is understandable in view of the high discharge utilization and hence, low neutral losses during the test.

But figures 16(a) and (b) do show that substantial direct-impingement erosion of the outermost grid apertures took place in the test. Since this same vector grid assembly had been used in several previous long duration tests at ΔV_I's near 40 volts without significant change in the direct-impingement erosion pattern, it must be concluded that the high ΔV_I caused substantial divergence and deflection of the outermost ion beamlets passing through the screen grid.

Though a weight change measurement was not obtained, the main cathode keeper (made of tantalum) suffered observable erosion over much of its downstream surface. This is evident from figure 17. Such erosion had not previously been observed during the extended tests of the SIT-5 thruster conducted at normal ΔV_I's using the same cathode and keeper.

Material Deposition and Flake Formation

On disassembly of the thruster after the accelerated life test, during which the thruster was oriented horizontally, copious large and small loose flakes were found on the lowest interior surfaces of the anode and the thruster body, particularly near their upstream ends. Figure 18 shows a portion of the flakes collected. With the scanning electron microscope the flakes were found to be typically 3 to 5 micrometers thick. Most were curled and some were as much as 1.0 millimeter long, though a typical length was more like 0.25 millimeter. Smaller loose flakes were also found on the anode pole-piece insert on the surfaces exposed to the main discharge. These flakes are seen in figure 19 as they appeared on disassembly of the thruster.

Nearly all of the loose flakes found in the thruster clearly originated from the spalling of sputtered material that had coated the smooth anode surfaces. Figure 20 indicates how extensive this spalling was. Indeed, the coating had apparently spalled completely from well over half of both the smooth tantalum foil anode insert surface and the exposed smooth anode shell surface.

Flaking of sputter-deposited material had also occurred from small areas on the upstream screen grid surface in or adjoining shadow-like areas extending radially outward from the 20 outermost screen grid holes (see fig. 21). These flakes were very small and probably would not have caused any operational problem even if they had migrated through or lodged elsewhere in the grid system. Evidently, increased net deposition of sputtered material had occurred in each shadow-like region, perhaps because of extraction through the adjacent grid hole of ions which otherwise would have sputtered this deposited material away.

Sputtered material also was visibly deposited on the thruster body interior over all of the unshielded area extending both upstream and downstream from the anode edges. This material did not show much tendency to spall, perhaps because it was unevenly distributed. The thickest deposits, which appeared rather lumpy, were concentrated in a narrow ring located even with the upstream edge of the anode. These deposits may be seen in figure 22. Such deposits also had been observed in the SIT-5 erosion tests (ref. 2). On microscopic examination, the thickest of these deposits did show raised broken edges and the potential for spalling as small flakes (fig. 23).

On disassembly of the thruster following the test, all of the loose flakes were brushed or shaken free, and all the coatings and deposits that were loose from but still attached to their substrates were removed by gentle scraping. The coatings then left on the parts involved were quite adherent and resistant to removal, except for the residual coating on the smooth portion of the tantalum foil anode insert, which is described later. (This residual coating was not removed.) The total weight of the flakes collected plus the loose material removed was 17.88 milligrams (table III). Some material that otherwise would have been included with the material weighed was lost during disassembly of the thruster and removal of the loose material from the thruster parts. This loss was judged to be <20 percent of the material weighed.

After all the loose material found was collected and removed from the thruster parts, the parts were weighed. Those showing weight gains and the amount of these gains are given in table III. The grid assembly, despite the deposited material identified earlier, showed a substantial overall weight loss, which is included in table II. A discrepancy (1.9 mg) between the measured weight gain of the anode-thruster body assembly, after the loose material and deposits had been removed, and the sum of the weight gains of the component parts after disassembly may be attributed to the loss of additional loose material during disassembly.

A comparison of the exposed grit-blasted and the smooth, virgin stainless-steel interior surfaces of the anode shell dramatically showed the difference in the adhesion of the sputtered discharge-chamber material to a smooth and to a roughened surface. The exposed grit-blasted surface (fig. 24) showed no flaws, cracks, or evidence of detached or attached flakes on microscopic examination. The exposed smooth, virgin sur-

face showed total spalling of the sputtered coating covering the downstream 60 percent of its surface (fig. 20) plus moderate spalling of the coating on the remainder of the exposed area.

The exposed grit-blasted and the smooth, virgin surface areas of the 0.05-millimeter-thick tantalum-foil anode insert showed the same difference in adhesion of the sputtered coating as did the stainless-steel anode shell. The whole interior surface of the insert is seen in figure 25. The coating on the grit-blasted surface was without cracks, flakes (attached or detached), or significant flaws. Its appearance on examination with the scanning electron microscope (fig. 26) is similar to that of the original grit-blasted surface except that the smaller surface features have been considerably smoothed and filled in. The original surface features have definitely not been obliterated, however, and the features of the coated surface have about the same typical surface dimension of 10 micrometers.

The coating on the smooth portion of the tantalum foil insert spalled off completely over the upstream 70 percent of its area. As seen in figures 25 and 27, the residual coating on the remaining area of the smooth surface showed a pronounced tendency to crack and spall into very large flakes with time and with the slight flexing unavoidable during disassembly and examination. No such cracking or spalling of the well-adhered coating on the adjacent grit-blasted surface of the insert occurred. Figure 28 shows how accurately the boundary of the spalled coating region coincided with the boundary between the smooth and the grit-blasted regions of the insert. This again indicates the predominant effect of the substrate surface roughness on the coating adhesion and spalling tendency.

The coarse screen anode insert showed no macroscopic spalling after the test. Examination of the screen insert with both optical and scanning electron microscopes revealed, however, that in a large number of cases the coating on the exposed screen wires was cracked along the crest of the wires, for a maximum length of one mesh unit. As seen in figure 29, many small flakes of less than one mesh unit length (0.50 mm) spalled or broke off from the edges of these cracks.

The stainless-steel anode mounting screws, which have exposed heads on the interior anode surface, showed a significant weight gain (table III) due to sputtered material deposited on their heads during the test. Examination following the test showed that this coating had partially spalled and peeled off from the heads in an irregular pattern.

The anode pole-piece insert gained a substantial amount of weight during the accelerated life test (table III). This was contrary to the weight losses experienced in the SIT-5 erosion studies (ref. 2), in which the pole-piece insert was used with its original smooth, nickel-plated surfaces. After the accelerated life test the pole-piece insert surfaces looked shinier than they had before the test. The weight gain and shinier sur-

faces may be attributable to the rough, granular, somewhat porous nature of the plasma-sprayed tantalum surfaces of the insert. These surfaces quite likely exhibited a much lower sputter yield than did the nickel surfaces in the SIT-5 tests and may also have had a significantly increased sticking coefficient for arriving sputtered material.

The possibility also exists that a small to substantial amount of mercury was sorbed by the porous tantalum surface of the insert, accounting for a direct weight gain and reducing to some extent the sputter erosion of the tantalum. Such behavior has been observed for graphite parts tested in the SIT-5 thruster (ref. 7). Finally, the possibility also exists that the much higher ΔV_I employed in the accelerated life test substantially altered the ion densities and trajectories in the region of the anode pole-piece insert, resulting in much reduced sputter erosion.

The substantial weight gain shown in table III for the cathode assembly shield also was in contrast to weight losses previously observed for this part in the SIT-5 erosion tests (ref. 2). The weight gain appeared to be due principally to a thin, adherent sputtered coating deposited on the exposed portion of the downstream surface in the test. The deposition of another, thinner coating on the upstream surface also was indicated, although inconclusively.

The material deposited on the downstream surface of the cathode assembly shield was doubtless sputtered principally from the upstream surface of the baffle and from the other exposed cathode pole-piece and baffle assembly surfaces located upstream of the baffle. The material, if any, deposited on the upstream surface of the cathode assembly shield must have been sputtered mainly from the downstream surface of the main cathode keeper. Both of these sputter erosion effects, as well as the weight gain of the cathode assembly shield, were unique to the accelerated life test, not having previously been observed in the SIT-5 erosion tests conducted at normal discharge potentials.

A reliable solution to the problem of anode coating deposition and spalling in small mercury-ion thrusters is apparent from the observations made of the anode surfaces after the accelerated life test. This solution is to use a coarsely grit-blasted screen anode surface of fine mesh size in conjunction with tantalum-surfaced discharge-chamber components (other than the molybdenum screen grid). At least up to substantial coating thicknesses, the sputtered material deposited under such conditions on this type of anode should be highly adherent, and, if any flakes of the coating should spall off, they should be limited in size to the screen mesh dimension. This may be chosen small enough so that the spalled flakes will not interfere with the operation of the thruster.

Sputtered Material Balance in Discharge Chamber

To obtain a total accounting of the component weight losses in the discharge chamber during the accelerated life test, the amount of weight lost from the upstream surface of the screen grid must be known. Unfortunately, this loss must be estimated from the total measured grid system weight loss because the screen grid could not be weighed directly. Such an estimate has been made in the same manner as in the SIT-5 erosion studies (ref. 2) by assuming that the screen grid experienced no net erosion or deposition other than on its upstream surface (in agreement with observation) and by also assuming the erosion of the accelerator grid elements to be proportional to the accelerator drain current J_A.

The accelerator grid system weight losses calculated in the SIT-5 erosion tests (ref. 2) have been used as the basis for such calculations in the present work because the identical electrostatic vector grid system was used in both studies. Thus, starting with the accelerator grid system weight loss (all assumed to be due to charge exchange ion erosion) calculated for the SIT-5 erosion test at $\Delta V_I = 42.6$ volts, multiplying by a factor of 200/407 to account for the relative duration of the two tests, and multiplying by another factor of 0.063/0.079 as the ratio of the base level constant J_A currents in the two tests, one obtains an estimate of 9.0 milligrams for the accelerator grid system weight loss due to charge-exchange ion erosion in the accelerated life test.

Significant direct-impingement erosion of the accelerator grid system was noted during the accelerated life test. An estimate of the weight loss resulting from this erosion may be made by associating the erosion with the observed decrease in J_A during the test to the final steady value shown in table I. (See footnote b of table I.) The result was multiplied by the ratio of the singly charged mercury ion (Hg^+) sputter yield on molybdenum at the ion energy of the direct-impingement ions ($\sim$2100 eV) to that yield at the ion energy of the charge-exchange ions ($\sim$700 eV). The sputter yields used are from Kemp and Hall (ref. 8). Finally, the ratio of the value just obtained to the total steady charge-exchange ion current integrated over the test was multiplied by the previously obtained estimate of 9.0 milligrams for the accelerator grid system weight loss due to charge-exchange ion erosion. The resulting estimate of the accelerator grid system weight loss due to direct-impingement ion erosion is 0.4 milligram. Hence, as shown in table II, the total estimated accelerator grid system weight loss from both direct-impringement and charge-exchange ion sputtering is 9.4 milligrams, and, by difference, the estimated weight eroded from the upstream surface of the screen grid is 90.1 milligrams.

With this estimate, the total of the discharge-chamber component weight losses in the accelerated life test comes to 215.7 milligrams (see table II). From table III the total of the discharge-chamber component weight gains plus the weight of the loose material collected from the discharge chamber interior amounts to 200.4 milligrams.

Hence, 93 percent of the estimated total weight loss is accounted for by the measured total weight gain, including the loose material collected. If the loose flakes and material lost on disassembly of the thruster could be accounted for, the weight loss and gain would be in even closer agreement.

The comparison of the total weight gained and the total weight lost in the accelerated-life test tends to substantiate the conclusion reached from the similar comparisons made in the SIT-5 erosion studies (ref. 2). This conclusion is that essentially all the material sputter-eroded from the discharge-chamber components ultimately deposits somewhere in the discharge chamber, principally on the anode. An almost negligible amount of sputtered material apparently is lost from the discharge chamber through the grid system. Likewise, with the thruster tested horizontally, a negligible amount of the flakes and other loose material generated in the discharge chamber during long-term operation passes into or through the grid system.

Sticking of Sputtered Material on Anode Surfaces; Spalling Processes

Careful estimates and calculations were made of the surface areas of the tantalum-foil anode insert, the screen anode insert, and the anode-shell interior which retained the sputtered coating deposited during the accelerated life test. This was done with all loose flakes and detached sections of the coating having previously been removed, in which condition the components also were weighed. The overall surface of the screen insert was assumed to be a sector of a smooth cylinder in calculating the coated area. From the measured weight gains and calculated coated areas of each of the three components, an average coating weight per unit coated area could be obtained. The results are presented in table IV.

The values for the coating weight per unit area are also compared in table IV, taking the value for the screen insert as the reference value. This was done on the assumption that a uniform sputtered coating of the same thickness covered all the coated areas of the three components. Inspection of the components showed this to be a good assumption. On this basis the results given in table IV indicate that the sputtered material in the accelerated life test showed the lowest deposition weight per unit coated area on the stainless-steel screen anode insert, a 23 percent higher value on the stainless-steel anode shell surfaces, and an 82 percent higher value for the tantalum anode insert than for the stainless-steel screen insert.

A partial explanation of the high ratio for the tantalum foil insert in table IV may be found in the appearance of the insert (fig. 25). This seems to indicate that the original coating on approximately the upstream 60 percent of the smooth portion of the insert spalled off completely during the latter stages of the test and a second coating, thin

enough to remain adherent, built up over this area during the remainder of the test. Since this area was not considered coated in the table IV calculations, the additional weight of the second coating would lead to a high result for the coating weight per unit coated area. However, it could not possibly account for all the difference observed in table IV between the results for the tantalum foil insert and the two stainless-steel components. The existence of a second coating on the tantalum foil insert is being investigated.

Another plausible, partial explanation of the high tantalum foil insert ratio in table IV lies in the fact that the full thickness residual coating that remained on the smooth portion of the insert when it was weighed was at the downstream end of the insert. In contrast, the residual coating on the smooth stainless-steel anode shell surface was at the upstream end. In both the SIT-5 erosion tests (ref. 2) and the 9715-hour SIT-5 endurance test (ref. 2), the sputtered coatings developed on the anode were over twice as thick at the downstream end as at the upstream end. If a similar variation in coating thickness with position on the anode applies to the accelerated life test (direct measurements of this coating thickness variation have not been made), the tantalum foil insert with its residual coating at the downstream end of the anode would show a higher coating weight per unit coated area than the other two anode surfaces in table IV. Again, however, this would not explain all the differences in the table IV results.

The comparatively low value in table IV for the coating weight per unit area on the stainless-steel screen insert is surprising for two reasons: (1) The actual exposed surface area of the insert was much larger than the area used in the calculations, since the latter was obtained by assuming a smooth cylindrical surface. (2) A substantial amount of the sputtered material that did not stick on its initial contact with the screen material deep in the screen meshes would be entrapped and deposited anyway because of the high probability that the rebounding sputtered molecules would strike and stick to another screen surface before escaping from the surface region of the screen insert. No satisfactory explanation of the comparatively low deposition weight per unit area on the screen insert is presently evident.

The curled condition of the flakes retrieved from the discharge chamber following the accelerated life test (fig. 18) suggests that residual forces, present in the coating when the thruster was shut down, were responsible for the spalling of the coating from the smooth anode surfaces and the generation of the observed flakes. Such forces could easily arise from a mismatch in the thermal expansion coefficients of the coating and the substrate, but other driving forces for the spalling from the smooth anode surfaces cannot be ruled out. It is clear, however, from the striking contrast between the coating adhesion to the smooth and the grit-blasted anode surfaces that the roughness of the anode surface has an effect on the coating adhesive forces considerably larger than the magnitude of the spalling forces present, at least for the anode coatings obtained and the thruster conditions prevailing in this work.

Apart from the case of the smooth tantalum foil anode insert surface, there was no other evidence of extensive spalling of the anode coating while the thruster actually was in operation. It appears quite likely that most of the remaining spalled flakes and loose material was generated as the thruster cooled following the life test. The only additional spalling observed after the thruster had been removed from the test facility was the spalling of more small flakes from the stainless-steel screen anode insert and the loosening of the remaining coating on the smooth portion of the tantalum foil anode insert (figs. 25 and 27). This loosening apparently resulted principally from slight flexing of the tantalum foil during disassembly and examination.

In the case of the smooth portion of the tantalum foil anode insert, the region of complete coating removal by spalling extended from the upstream edge; in the case of the smooth exposed surface of the anode shell, it extended from the downstream edge. This inconsistency in the location of total coating spalling, together with the other observations described previously, is in agreement with the conclusion previously reported (ref. 2) that the spalling of a sputter-deposited coating from a smooth anode surface is not a function principally of a single variable or a simple combination of variables from amongst the coating thickness, coating composition, substrate composition, and location on the anode.

Acceleration of Sputter Erosion and Deposition

The only two discharge-chamber components common to both the accelerated life test and the SIT-5 erosion tests were the tantalum baffle and the molybdenum screen grid (the screen grid as part of the electrostatic vector grid system). Other parts used in the SIT-5 erosion studies, including the anode pole-piece insert, the cathode pole piece, and the thruster endplate, were also used in the accelerated life test but with tantalum coatings or covers on their exposed surfaces. Hence, comparison of the erosion rates of common thruster components between the SIT-5 tests and the accelerated life test is limited to the baffle and the screen grid.

The baffle support system used in the accelerated life test was considerably altered from that used in the SIT-5 erosion tests, as noted before. In spite of these changes, the exposed surface area of the baffle on both its downstream and upstream sides, as well as the position of the baffle relative to the cathode pole piece, was nearly the same in both experiments. Neglecting any differences in exposed surface area, position, or sputtering processes, the same baffle showed a weight erosion rate 74.1 times greater in the accelerated life test than it did (ref. 2) during the 416-hour SIT-5 erosion test at the standard ΔV_I of 39.6 volts.

The estimated erosion of the screen grid upstream surface during the accelerated life test may be compared with that estimated in the SIT-5 erosion studies, since both estimates were made from the measured total grid system weight losses by the same procedure. Such a comparison indicates a weight erosion rate 75 times greater in the accelerated life test than during the 416-hour SIT-5 test at $\Delta V_I = 39.6$ volts.

This close agreement between the factors by which the sputter erosion rates of two different discharge-chamber components were increased in the accelerated life test is coincidental in view of the uncertainties in both comparisons. Yet it does permit the inference that the sputter-erosion damage suffered by the discharge-chamber components in the 200-hour accelerated life test, as well as the deposition of sputtered material which took place in the test, was equivalent to that which would occur during approximately 15 000 hours of continuous operation at a normal ΔV_I of 39.6 volts.

Convincing evidence was obtained in the SIT-5 erosion studies (ref. 2) that Hg^{+2} ions were the species predominantly responsible for the observed sputter erosion of the discharge-chamber components. This conclusion was partially deduced from the fact that the relative erosion rates found over the investigated range of ΔV_I (36.6 to 42.6 V) could be well correlated with the variation in the Hg^{+2} ion production rate predicted over the same ΔV_I range. The predicted production rate curve was obtained from the Gryzinski semitheoretical formulation (ref. 2) for the one important Hg^{+2} production reaction:

$$Hg^{+} + e^{-} \rightarrow Hg^{+2} + 2e^{-}$$

(In this reaction both the Hg^{+} and the Hg^{+2} ions are in their ground states and the bombarding electron (e^{-}) removes only the remaining s electron of the Hg^{+} ion.)

This type of analysis may be extended to $\Delta V_I = 64.6$ volts, at which ΔV_I the reaction given is still expected to be the predominant source of Hg^{+2} ions. If this is done, it is found from figure 21 of reference 2 plus appropriate sputter yield data (ref. 9) that only an increase of approximately 24 times in the sputter erosion rates at $\Delta V_I = 64.6$ volts from those at 39.6 volts can be explained on the basis of increased Hg^{+2} ion production from the indicated reaction. (This computation includes the effects of the increased Hg^{+2} ion sputter yields at the higher ΔV_I.)

Because the sputter erosion rates in the accelerated life test were actually increased by factors of about 75, clearly another sputtering agent or new production reactions must play an important role in the sputter erosion occurring when the ΔV_I is raised to 65 volts. Other reactions that would produce additional Hg^{+2} ions at the higher ΔV_I are insufficient to explain the observed effect unless substantial changes in the main discharge also occur, such as in the ratio of primary to Maxwellian electrons.

A likely explanation of at least a significant portion of the unexpectedly large erosion rates observed at $\Delta V_I = 64.6$ volts is that at this ΔV_I significant production of and sputter erosion by triply charged mercury ions (Hg^{+3}) takes place. The threshold primary electron energy required for production of Hg^{+3} from Hg^{+2} ions corresponds to a ΔV_I of ~49 volts, and at a ΔV_I of approximately 65 volts the Hg^{+3} production cross sections are indicated by Gryzinski calculations to be substantial (private communication from P. J. Wilbur of Colorado State Univ.). Furthermore, the sputter yields of the Hg^{+3} ions at a ΔV_I of 65 volts are expected to be considerably increased from those of the Hg^{+2} and Hg^{+} ions at this ΔV_I because of the approximately 195-electron-volt sputtering energy of the Hg^{+3} ions. This combination of factors means that a relatively small number density of Hg^{+3} ions produced at the high ΔV_I could be responsible for a substantial proportion of the high sputter erosion rates observed in the accelerated life test. Detailed calculations or data supporting this explanation, however, are not yet available.

The hypothesis that Hg^{+3} ion erosion was important in the accelerated life test probably does not offer a reasonable explanation of the observed erosion of the upstream surface of the baffle and that of the cathode keeper, accompanied by the apparent deposition of much of this material on the cathode assembly shield. This erosion is more likely the result of significant Hg^{+2} ion production in the cathode-baffle region due to the penetration into this region of plasma potentials sufficiently high to create primary electrons with energies above the Hg^{+2} production reaction threshold of 18.75 electron volts (ref. 10). The relative absence of erosion upstream of the baffle in the SIT-5 erosion tests indicates that such plasma potentials do not exist in the cathode-baffle region when the thruster is operated at normal ΔV_I's around 40 volts.

Despite the qualitative erosion differences between the SIT-5 erosion tests and the accelerated life test and, despite the possible importance only in the accelerated life test of sputtering by Hg^{+3} ions, the close similarities observed in the sputter-erosion and deposition results of the experiments remain clear. These include the predominant erosion of the cathode pole piece (especially the tip), the baffle assembly (on its downstream side), and the screen grid (upstream surface) and the nearly total deposition of this sputtered material on the anode and adjacent surfaces.

This observed qualitative similarity in the overall erosion and deposition features, together with the agreement found in the sputter-erosion-rate acceleration for two widely separated discharge-chamber components, supports the validity of the accelerated-life test concept. A relatively short operational test of a small mercury-ion thruster conducted at an elevated ΔV_I thus appears able to approximately reproduce the major sputter erosion, deposition, and anode deposit spalling effects that occur in the discharge chamber of such a thruster during normal, uncycled operation for periods in the range of 10 000 to 20 000 hours.

SUMMARY OF RESULTS

A 200-hour operational test conducted on a modified SIT-5 thruster at a discharge potential ΔV_I of 64.6 volts, with otherwise standard SIT-5 operating conditions, reproduced the major sputter erosion and deposition effects estimated to occur in the discharge chamber in 15 000 hours of uncycled operation at a standard ΔV_I of 40 volts.

The anode deposits generated were very adherent to grit-blasted tantalum and stainless-steel anode surfaces and moderately adherent to a coarse stainless-steel screen on the anode. These results were obtained with essentially all the sputter eroded discharge-chamber components in the thruster covered with, coated with, or constructed of tantalum, apart from the molybdenum screen grid. No spalling of the anode coating from the grit-blasted surfaces occurred, and, from the stainless-steel screen anode surface spalling only of minute coating flakes, less than one screen mesh unit long, was observed.

The discharge-chamber erosion and deposition rates were accelerated by a factor of approximately 75 at a ΔV_I of 64.6 volts, as compared with the rates previously found under normal operation at 39.6 volts. The agreement between the acceleration factor calculated from the estimated erosion of the screen grid and that calculated from the measured erosion of the baffle was excellent.

Sputter erosion of the cathode pole piece, baffle, and baffle screw in the modified SIT-5 thruster tested does not threaten the structural integrity and serviceability of these components for at least several times the 15 000 equivalent hours of normal uncycled thruster operation represented by the accelerated life test. The small dimensional losses of these components due to sputter erosion during the test may have been related to observable changes noted in the thruster operating characteristics, but they had no critical effect on these characteristics.

Use of a grit-blasted, fine-mesh-screen anode surface, in conjunction with the use of tantalum for the exposed surfaces of all the other discharge-chamber components except the molybdenum screen grid, is indicated as satisfactorily solving the problems of discharge-chamber sputter erosion and anode deposit spalling in small mercury ion thrusters for operational life times in excess of 15 000 hours. The anode coating produced with these thruster modifications should be highly adherent, and any flakes spalling from it should be limited in size to the screen mesh dimension. Hence, such flakes should be innocuous to the thruster operation provided the screen mesh is chosen sufficiently fine.

The discharge-chamber component weight gains, together with the loose flakes collected, accounted for at least 93 percent of the total discharge-chamber component weight losses found in the accelerated life test. This weight balance is in agreement with the previously reported conclusion that essentially all the material sputtered from

the discharge-chamber components during thruster operation deposits elsewhere in the discharge chamber, principally on the anode.

The extensive spalling of anode deposit flakes from the smooth tantalum and stainless-steel anode surfaces in the accelerated life test demonstrates the extreme bonding weakness of sputter-deposited anode coatings to smooth surfaces and the ease with which residual forces in the coatings can cause their detachment from such substrates.

Stable and smooth thruster operation was obtained during the accelerated life test with automatic control of the main vaporizer based on the sensing of $(\Delta V_I - V_{CK})$ (where V_{CK} is the cathode keeper potential), instead of ΔV_I as in the standard thruster control circuit. This experience suggests the general desirability of main cathode flow control based on $(\Delta V_I - V_{CK})$ in small mercury ion thrusters. Such control eliminates mercury flow perturbations caused by cathode keeper discharge fluctuations.

Lewis Research Center,
National Aeronautics and Space Administration,
Cleveland, Ohio, January 31, 1975,
506-22.

REFERENCES

1. Nakanishi, S.; and Finke, R. C.: A 9700-Hour Durability Test of a Five Centimeter Diameter Ion Thruster. AIAA Paper 73-1111, Oct.-Nov. 1973.

2. Power, J. L.: Sputter Erosion and Deposition in the Discharge Chamber of a Small Mercury Ion Thruster. AIAA Paper 73-1109, Oct.-Nov. 1973.

3. Hyman, Julius, Jr.: Performance Optimized, Small Structurally Integrated Ion Thruster System. (Hughes Research Labs.) NASA CR-121183, 1973.

4. Hyman, J., Jr.: SIT-5 System Development. AIAA Paper 72-492, Apr. 1972.

5. Hudson, W. R.; and Banks, B. A.: An 8-cm Electron Bombardment Thruster for Auxiliary Propulsion. AIAA Paper 73-1131, Oct.-Nov. 1973.

6. Bechtel, Robert B.: Component Testing of a 30-Centimeter-Diameter Electron Bombardment Thruster. AIAA Paper 70-1100, Aug.-Sept. 1970.

7. Banks, B. A.: 8-Cm Mercury Ion Thruster System Technology. AIAA Paper 74-1116, Oct. 1974.

8. Kemp, Robert F.; and Hall, David F.: Ion Beam Diagnostics and Neutralization. (TRW-06188-6011-R000, TRW Systems Group; NAS3-7937.) NASA CR-72343, 1967.

9. Askerov, Sh. G.; and Sena, L. A.: Cathode Sputtering of Metals by Slow Mercury Ions. Fiz. Tverd. Tela, vol. 11, no. 6, June 1969 pp. 1591-1597.

10. Milder, Nelson L.; and Sovey, James S.: Characteristics of the Optical Radiation from Kaufman Thrusters. NASA TN D-6565, 1971.

TABLE I. - CHARACTERISTIC THRUSTER OPERATING CONDITIONS

Discharge potential, ΔV_I, V	64.6
Ion-beam accelerating potential,[a] $(V_I + V_G)$, V	1393
Accelerator potential, V_A, V	-700
Neutralizer coupling potential, V_G, V	-14
Beam current, J_B, mA	23.4
Accelerator drain current, J_A, mA	[b]0.063
Emission current, J_E, mA	[c]372
Cathode mercury flow rate, $\dot{m}_c$, equivalent mA	29.9
Neutralizer mercury flow rate, $\dot{m}_N$, equivalent mA	14.7
Cathode keeper potential, V_{CK}, V	[d]15
Neutralizer keeper potential, V_{NK}, V	[e]18
Cathode keeper current, J_{CK}, mA	400
Neutralizer keeper current, J_{NK}, mA	360
Cathode tip heater power, W	0
Neutralizer tip heater power, W	0
Discharge utilization,[f] percent	78.2
Discharge losses,[g] eV/ion	1027
High voltage on time, hr	200
Discharge on time, hr	200

[a]Equal to net accelerating potential V_I plus neutralizer coupling potential V_g (<0).

[b]Steady value latter part of test; initial value, 0.078 mA.

[c]Typical value; ranged from 342 mA at beginning of test to 396 mA at end.

[d]Rapid fluctuations to 17 to 19 V throughout test.

[e]Value near end of test; steady rise from initial 14-V value during test.

[f]Neglecting double ionization.

[g]Excluding cathode keeper losses and neglecting double ionization.

TABLE II. - WEIGHT LOSSES IN ACCELERATED LIFE TEST

Component	Initial weight, g	Weight loss, mg	
Cathode pole-piece and baffle assembly[a]	12.2	------	120.17
Cathode pole piece[b]	10.9	11.44	------
Cathode pole-piece tip cover	.182	59.48	------
Cathode pole-piece outer flange cover	.561	14.54	------
Baffle	.267	25.63	------
Baffle screw	.110	8.77	------
Baffle washer	.0380	.39	------
Baffle nut	.121	1.04	------
Total for cathode pole-piece and baffle assembly components		121.29	
Cathode pole piece screws	.0901	------	.10
Endplate cover	16.2	------	5.37
Electrostatic vector grid assembly	155	99.5	------
Estimate for accelerator grid system[c]	--------	-9.4	------
Estimate for screen grid[d]	--------	90.1	90.1
Total losses of discharge chamber components[e]	--------	------	215.7

[a]Weighed as unit with pole piece covers installed but not including cathode pole-piece screws.

[b]Without pole-piece covers.

[c]Includes both charge exchange and direct impingement ion sputtering - see text.

[d]Upstream (discharge chamber) surface.

[e]Sum of cathode pole-piece and baffle assembly loss, cathode pole-piece screw losses, endplate cover loss, and estimated screen grid loss.

TABLE III. - WEIGHT GAINS AND LOOSE MATERIAL

COLLECTED IN ACCELERATED LIFE TEST

Component	Initial weight, g	Weight gain, mg	
Anode-thruster body assembly[a]	48.3		161.82
Thruster body[a]	26.9	9.96	------
Anode shell[a]	6.44	28.91	------
Screen anode insert	8.03	61.34	------
Tantalum foil anode insert[b]	1.83	58.59	------
Anode mounting screws	1.43	1.15	------
Anode interior mounting insulators and shadow shields	1.36	0	------
Total for anode-thruster body assembly components[a, c]		159.94	------
Cathode assembly shield	5.35	------	9.06
Endplate[d]	43.7	------	.67
Anode pole-piece insert	7.75	------	10.94
Loose material collected	-----	------	17.88
Total of component weight gains and loose material collected[e]	-----	------	200.38

[a]Loose material removed.

[b]Loose material initially removed; residual coating which later loosened from substrate not removed. (See text.)

[c]Includes components listed plus anode mounting hardware outside of discharge chamber, which showed a 0.01-mg weight loss in test.

[d]Interior surface exposed only through four screw holes in cathode pole piece.

[e]Sum of anode-thruster body assembly gain (corrected for external hardware weight loss, see note c), cathode assembly shield gain, endplate gain, and anode pole piece insert gain, plus weight of loose material collected.

TABLE IV. - WEIGHT GAIN PER UNIT AREA

FOR COATED ANODE SURFACES

Anode surface	Weight gain, mg	Coated area,[a] cm^2	Weight gain per unit coated area, mg/cm^2	Ratio relative to screen insert
Stainless steel screen insert	61.34	24.8[b]	2.48	1.00
Stainless steel shell	28.91	9.46[c]	3.06	1.23
Tantalum foil insert	58.59	13.0[c]	4.50	1.82

[a]When weighed. See text.

[b]Assuming surface to be sector of smooth cylinder.

[c]Including coated area of both smooth and grit-blasted surfaces.

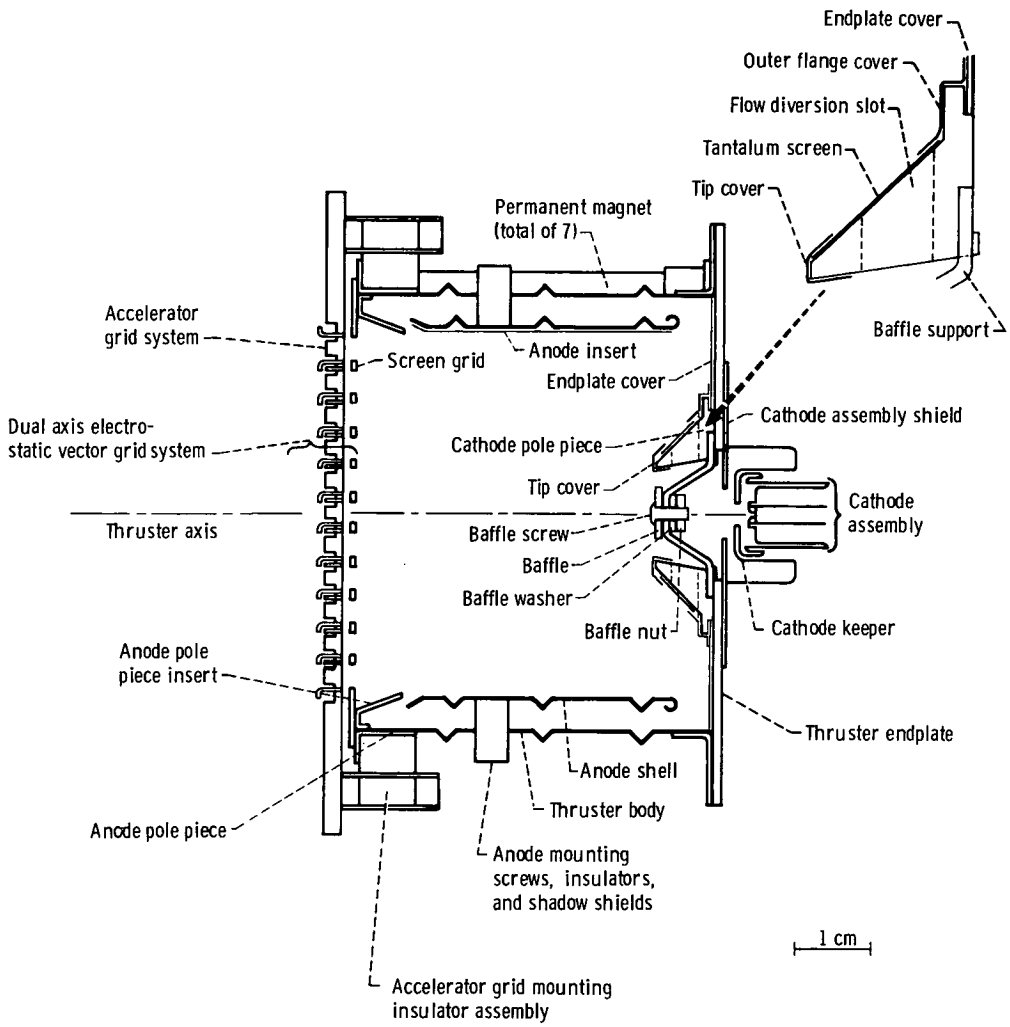

Figure 1. - Sectional view of modified 5-centimeter thruster used in accelerated life test. Neutralizer and ground screen not shown.

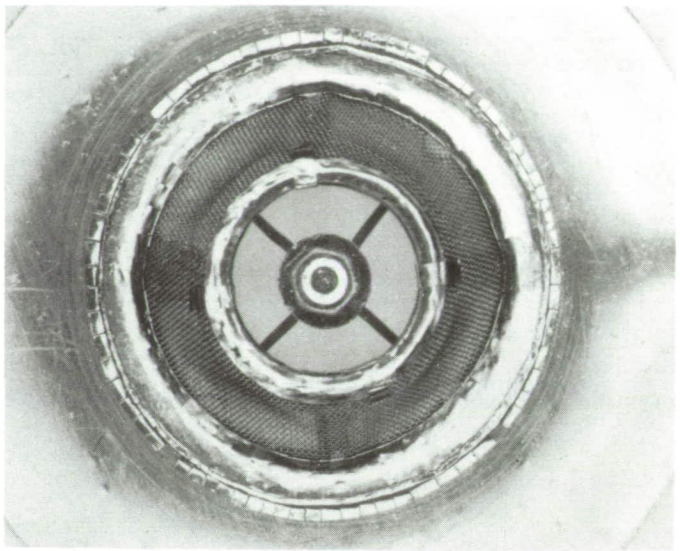

Figure 2. - Cathode pole-piece and baffle assembly, before test, showing pole-piece tip and outer flange tantalum foil covers.

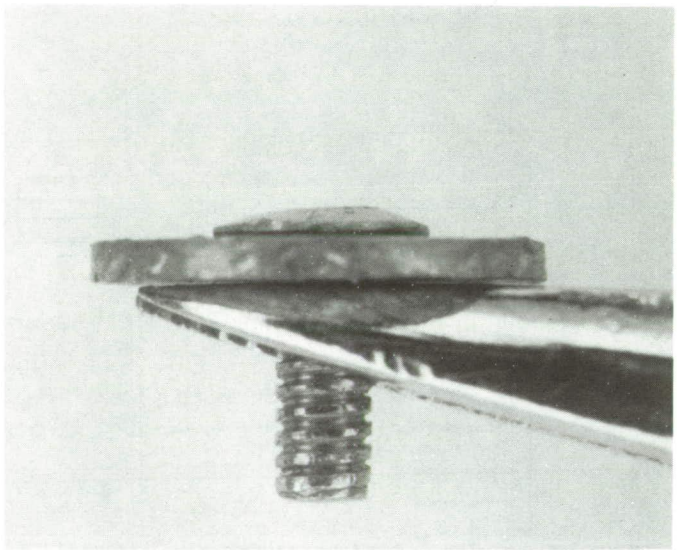

Figure 3. - Tantalum baffle and baffle screw before test.

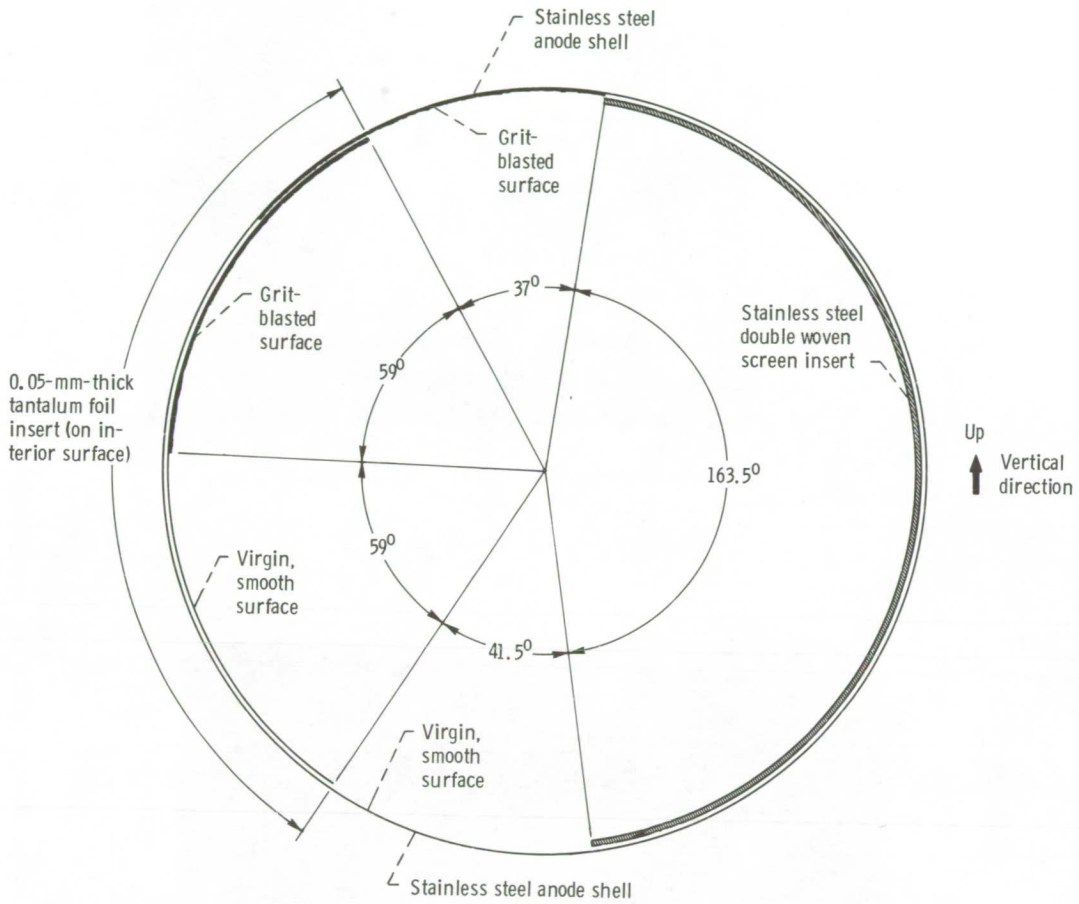

Figure 4. - Layout of composite anode (looking upstream).

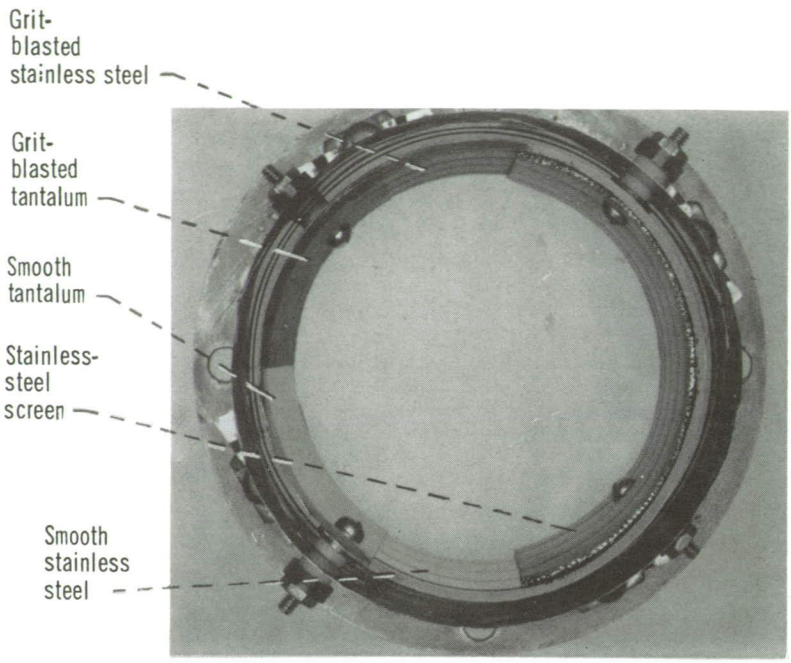

Figure 5. - Composite anode-thruster body assembly, looking upstream, before test.

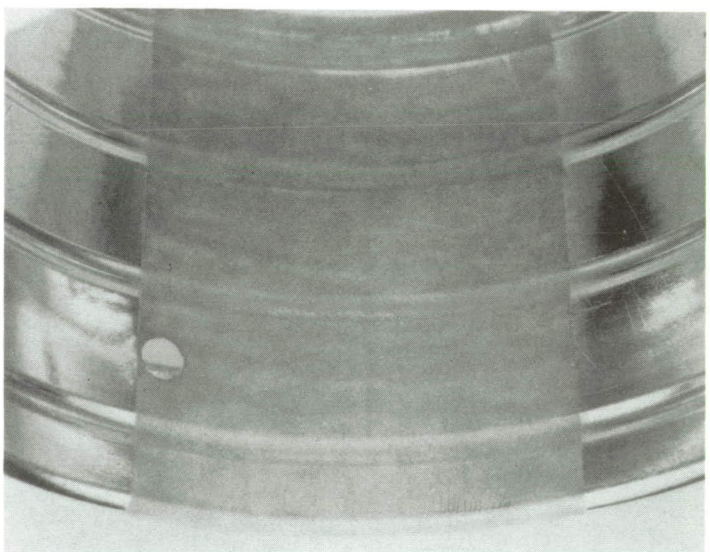

Figure 6. - Grit-blasted interior anode shell surface before test.

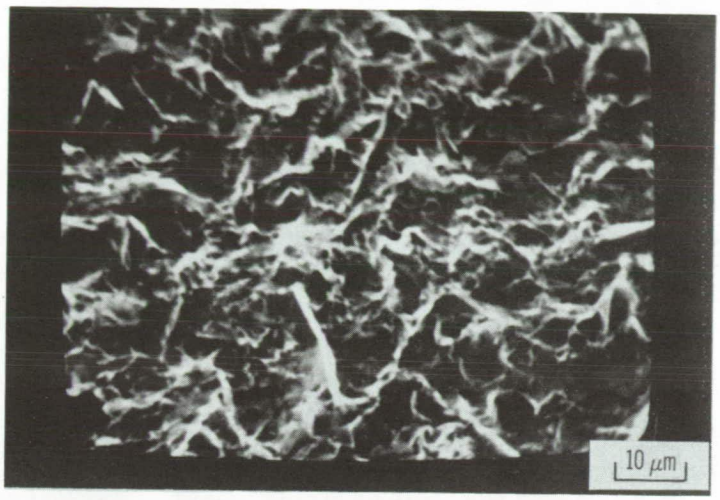

Figure 7. - Electron micrograph of grit-blasted stainless-steel anode shell surface before test.

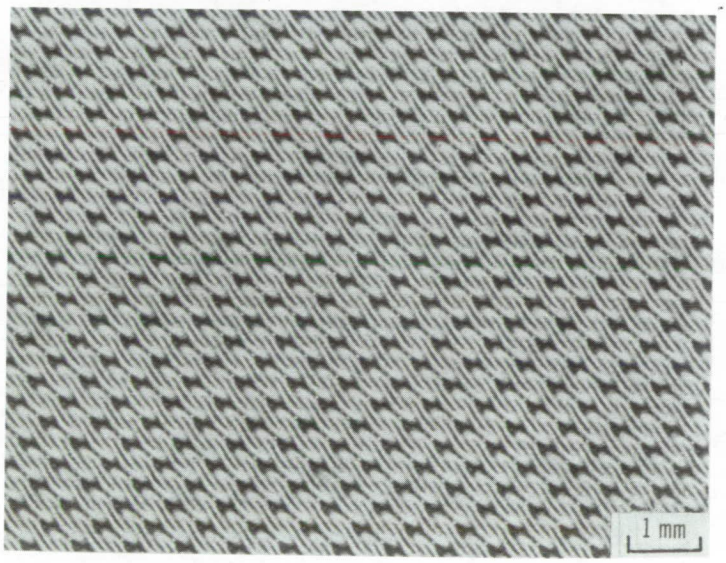

Figure 8. - Stainless-steel screen anode insert before test.

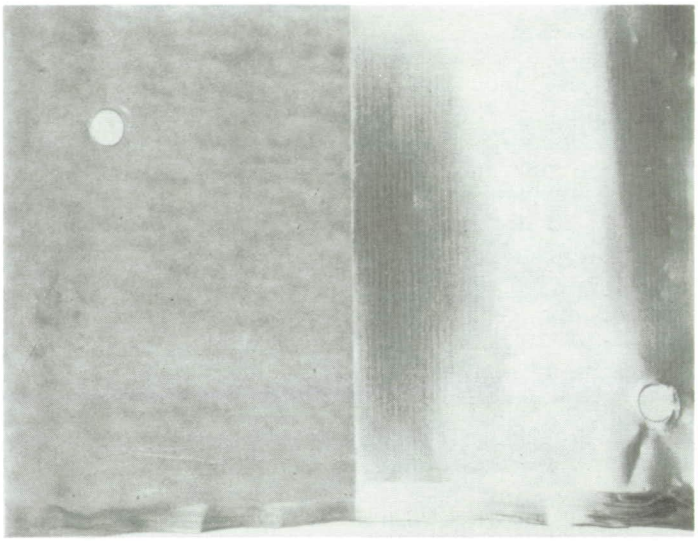

Figure 9. - 0.05-Millimeter-thick tantalum foil anode insert before test. Grit-blasted surface on left; downstream edge at bottom.

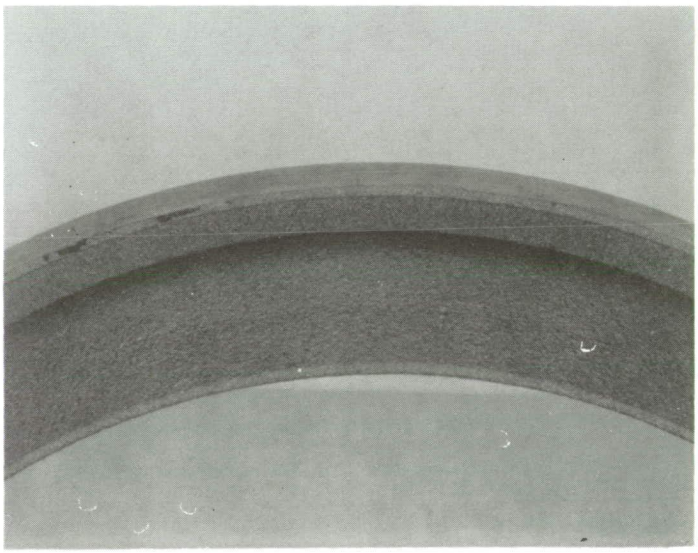

Figure 10. - Anode pole-piece insert (before test), showing tantalum plasma-sprayed interior upstream surfaces.

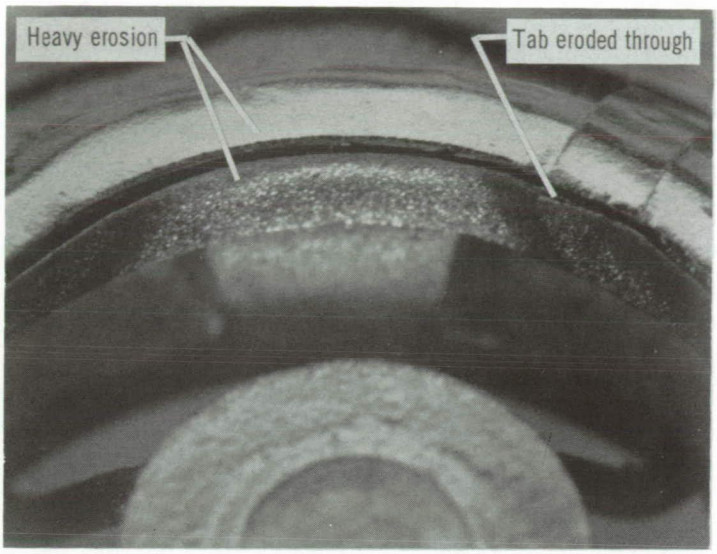

Figure 11. - Cathode pole-piece tip cover (0.05-mm-thick tantalum foil) after test; baffle in foreground.

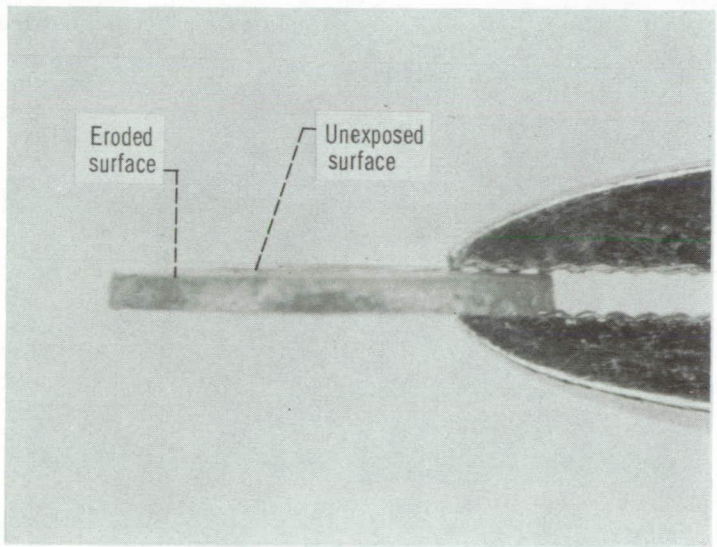

Figure 12. - Tantalum baffle edge view after test; downstream surface up.

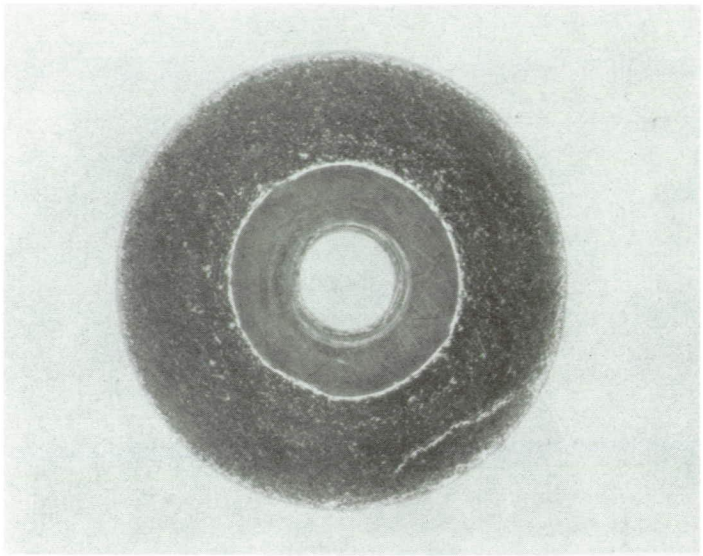

Figure 13. - Downstream surface of tantalum baffle after test; central area covered by baffle screw head.

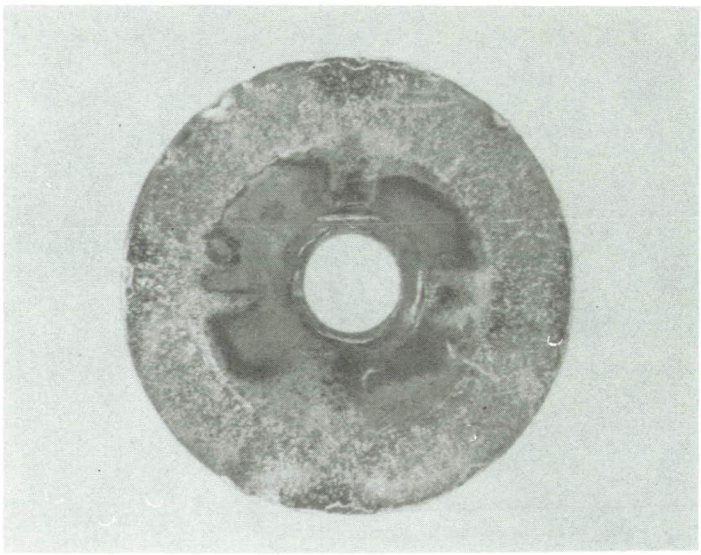

Figure 14. - Upstream surface of tantalum baffle after test.

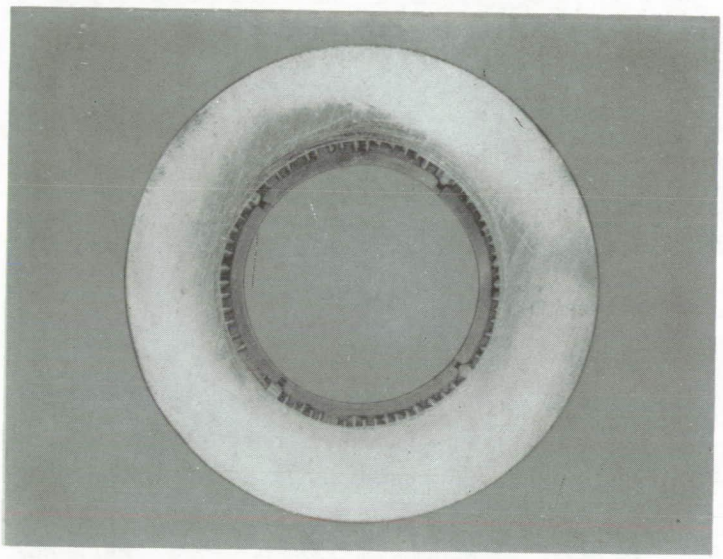

Figure 15. - 0.50-Millimeter-thick tantalum endplate cover after test; central area covered by cathode pole piece.

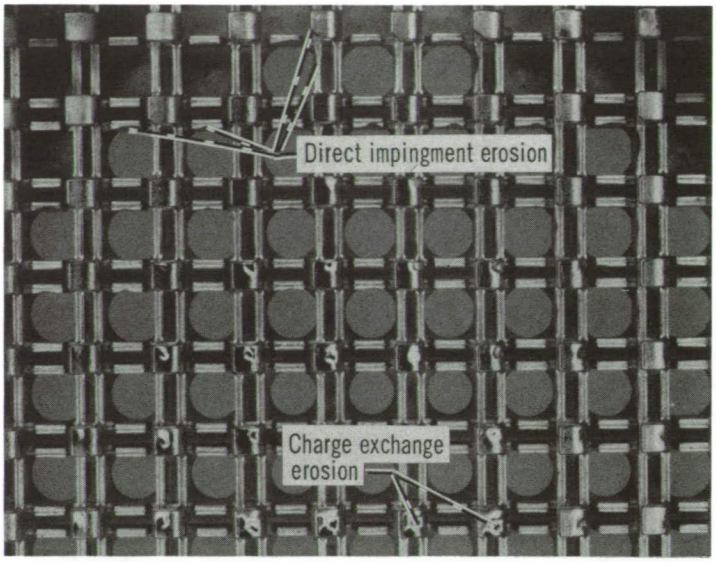

(a) Before test.

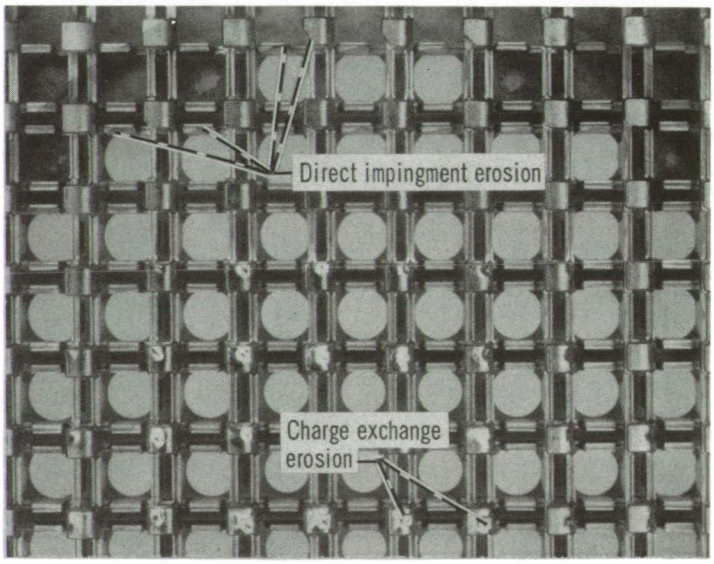

(b) After test.

Figure 16. - Portion of electrostatic vectoring accelerator grid system, showing direct impingement and charge-exchange erosion.

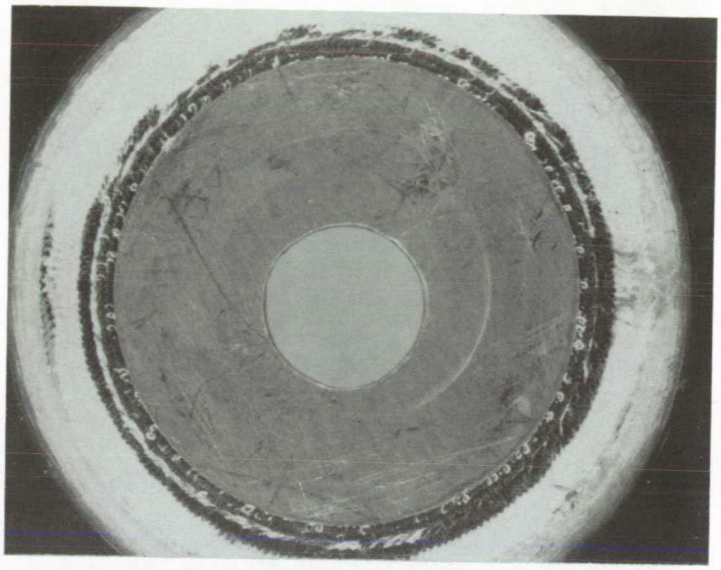

(a) Before test.

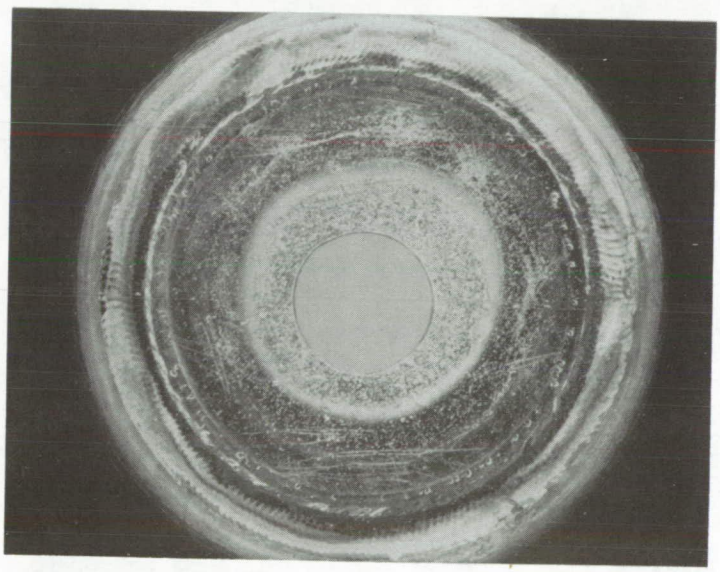

(b) After test.

Figure 17. - Downstream surface of main cathode keeper (tantalum).

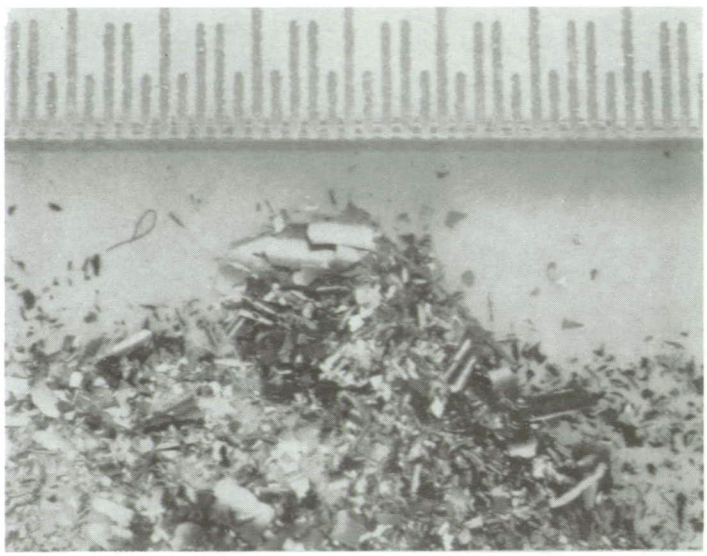

Figure 18. - Portion of loose flakes and material collected from thruster discharge chamber after test. Smallest divisions on ruler, each 0.254 millimeter (0.01 in.).

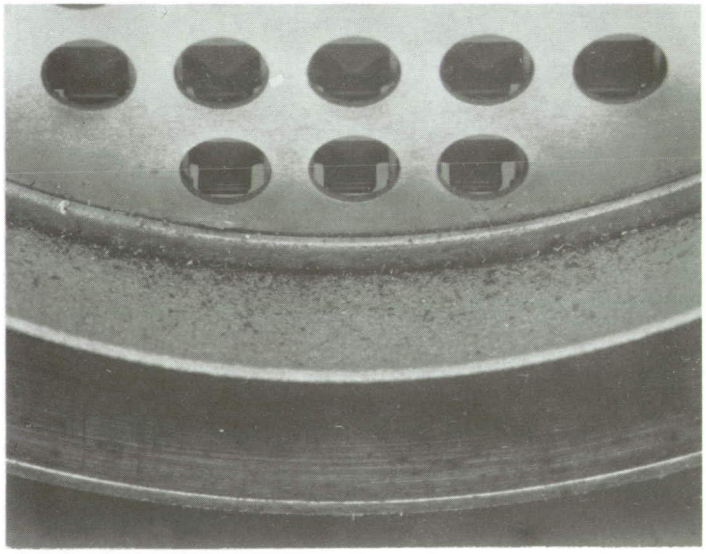

Figure 19. - Interior surfaces of anode pole-piece insert and screen grid on disassembly of thruster after test, showing loose flakes.

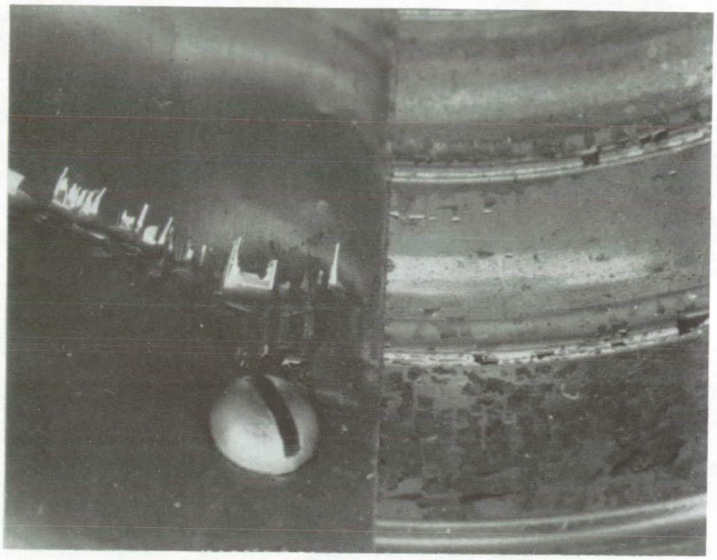

Figure 20. - Interior of anode assembly after test, looking upstream. Smooth tantalum foil insert surface on left; smooth stainless-steel anode shell surface on right.

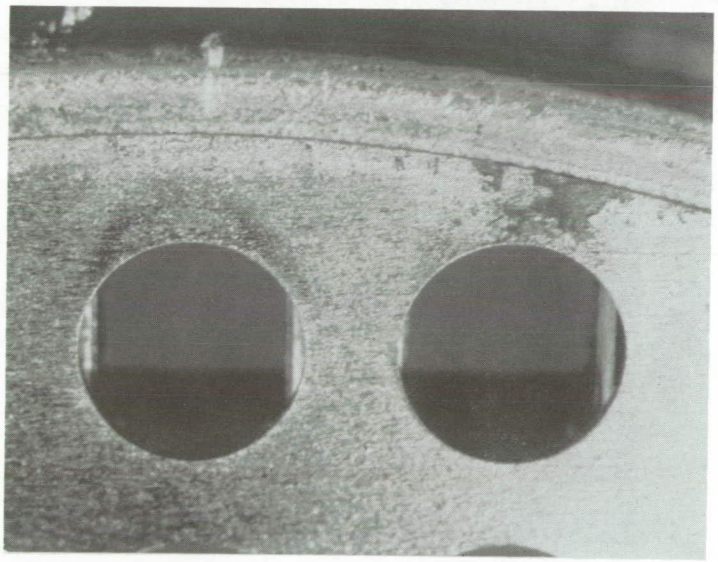

Figure 21. - Outer perimeter of screen grid upstream surface, showing loose and detached coating.

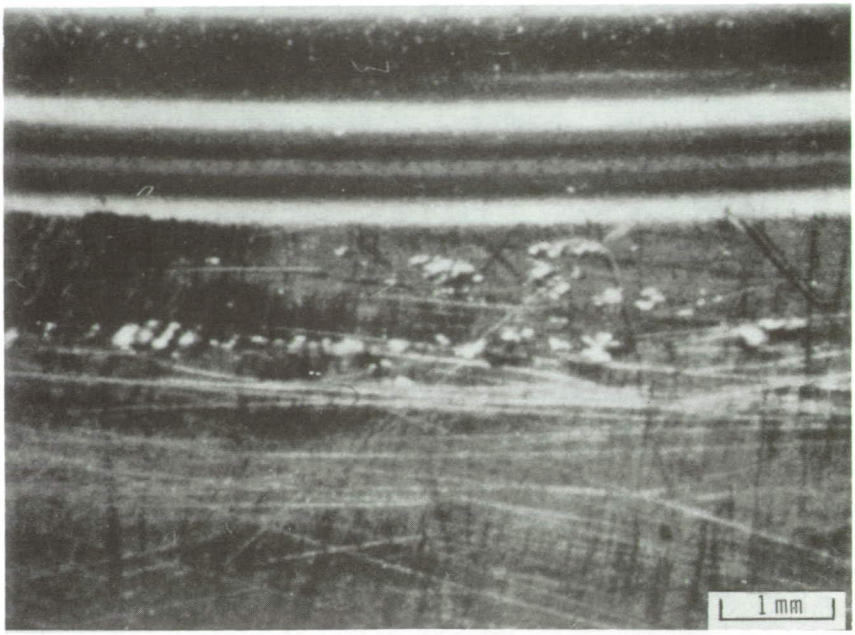

Figure 22. - Interior thruster body surface near upstream end after test. Note lumpy deposits.

Figure 23. - Photomicrograph of deposits near upstream end of thruster body interior surface after test.

Figure 24. - Grit-blasted interior anode shell surface after test. Section at left not exposed to discharge.

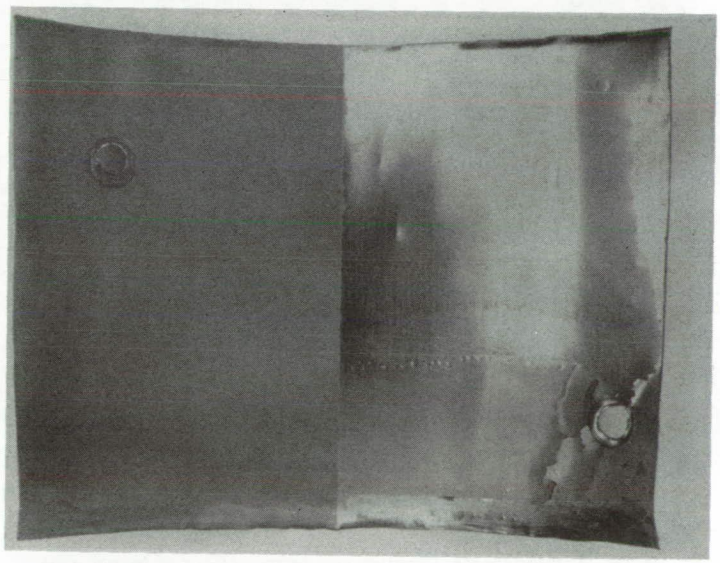

Figure 25. - Tantalum foil anode insert after test. Grit-blasted surface on left; downstream edge at bottom.

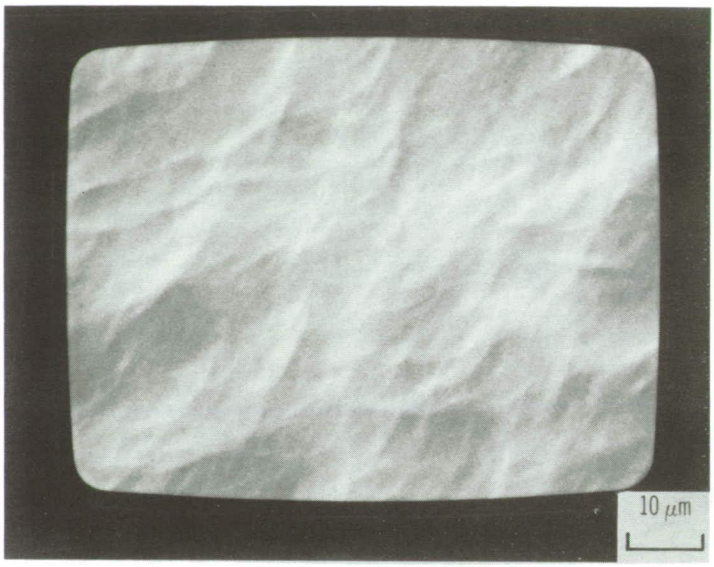

Figure 26. - Electron micrograph of coated, grit-blasted surface of tantalum foil anode insert after test.

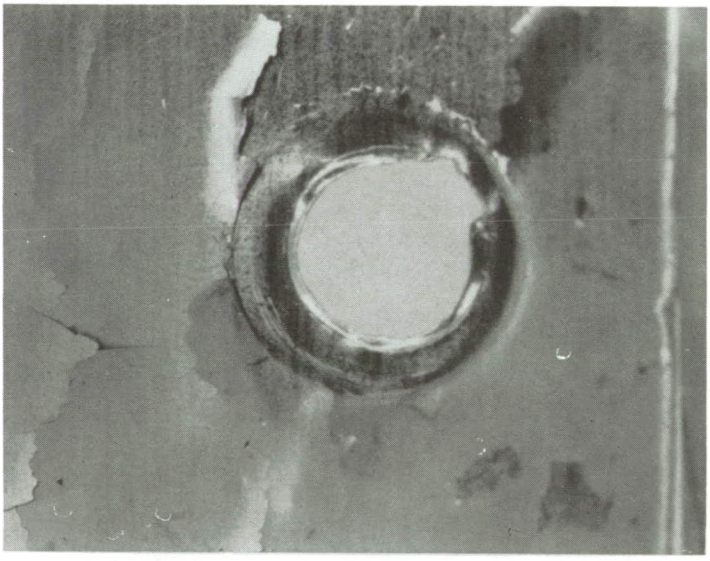

Figure 27. - Spalled residual coating on smooth surface of tantalum foil anode insert near downstream edge after test.

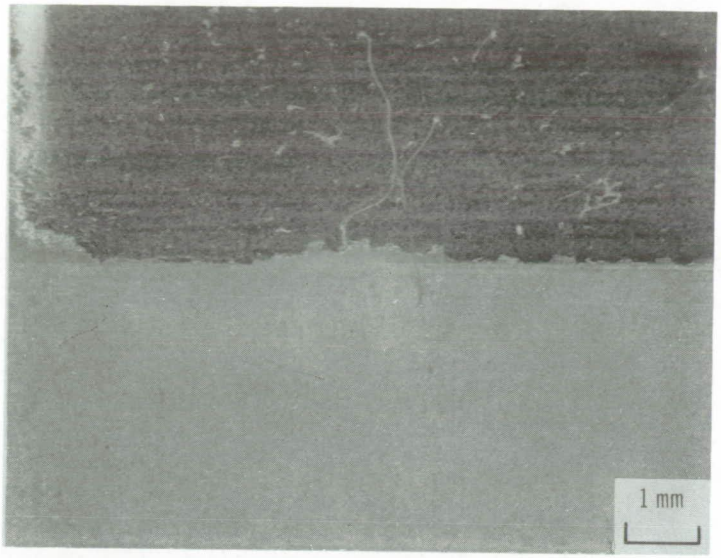

Figure 28. - Tantalum foil anode insert (after test), showing coated grit-blasted surface (at bottom) and smooth surface with coating spalled off (at top), near upstream edge.

Figure 29. - Electron micrograph of stainless-steel screen anode insert (after test), showing spalled coating areas and cracks.

NATIONAL AERONAUTICS AND SPACE ADMINISTRATION
WASHINGTON, D.C. 20546

OFFICIAL BUSINESS
PENALTY FOR PRIVATE USE $300

SPECIAL FOURTH-CLASS RATE BOOK

POSTAGE AND FEES PAID
NATIONAL AERONAUTICS AND SPACE ADMINISTRATION
451

U.S.MAIL

POSTMASTER: If Undeliverable (Section 158 Postal Manual) Do Not Return

"The aeronautical and space activities of the United States shall be conducted so as to contribute . . . to the expansion of human knowledge of phenomena in the atmosphere and space. The Administration shall provide for the widest practicable and appropriate dissemination of information concerning its activities and the results thereof."

—NATIONAL AERONAUTICS AND SPACE ACT OF 1958

NASA SCIENTIFIC AND TECHNICAL PUBLICATIONS

TECHNICAL REPORTS: Scientific and technical information considered important, complete, and a lasting contribution to existing knowledge.

TECHNICAL NOTES: Information less broad in scope but nevertheless of importance as a contribution to existing knowledge.

TECHNICAL MEMORANDUMS: Information receiving limited distribution because of preliminary data, security classification, or other reasons. Also includes conference proceedings with either limited or unlimited distribution.

CONTRACTOR REPORTS: Scientific and technical information generated under a NASA contract or grant and considered an important contribution to existing knowledge.

TECHNICAL TRANSLATIONS: Information published in a foreign language considered to merit NASA distribution in English.

SPECIAL PUBLICATIONS: Information derived from or of value to NASA activities. Publications include final reports of major projects, monographs, data compilations, handbooks, sourcebooks, and special bibliographies.

TECHNOLOGY UTILIZATION PUBLICATIONS: Information on technology used by NASA that may be of particular interest in commercial and other non-aerospace applications. Publications include Tech Briefs, Technology Utilization Reports and Technology Surveys.

Details on the availability of these publications may be obtained from:

SCIENTIFIC AND TECHNICAL INFORMATION OFFICE

NATIONAL AERONAUTICS AND SPACE ADMINISTRATION

Washington, D.C. 20546